

The Protophobic Light Vector Boson as a Mediator to the Dark Sector

Tepei Kitahara^{1,2,*} and Yasuhiro Yamamoto^{3,†}

¹*Institute for Theoretical Particle Physics (TTP), Karlsruhe Institute of Technology,
Wolfgang-Gaede-Straße 1, 76128 Karlsruhe, Germany*

²*Institute for Nuclear Physics (IKP), Karlsruhe Institute of Technology,
Hermann-von-Helmholtz-Platz 1, 76344 Eggenstein-Leopoldshafen, Germany*

³*Department of Physics, Osaka University, Toyonaka 560-0043 Osaka, Japan*

(Dated: September 7, 2016)

Observation of a protophobic 16.7 MeV vector boson has been reported by a ^8Be nuclear transition experiment. Such a new particle could mediate between the Standard Model and a dark sector which includes the dark matter. In this Letter, we show some simple models which satisfy the thermal relic abundance under the current experimental bounds from the direct and the indirect detections. In a model, it is found that an appropriate self-scattering cross section to solve the small scale structure puzzles can be achieved.

PACS numbers: 95.35.+d, 27.20.+n, 21.30.-x, 12.60.-i

INTRODUCTION

Although the dark matter has been gravitationally confirmed by astrophysical observations in various way, one has no information on the properties, e.g., the mass and the coupling. In a various dark matter models, a kind of popular model includes a light new boson which mediates between the Standard Model and a dark sector, e.g., Ref. [1]. Such a light particle simultaneously plays an important role in order to solve several problems, for instance, the small scale structure problems [2], the Lithium problem [3], and the muon $g-2$ anomaly [4].

Recently, a ^8Be nuclear transition experiment has reported a signal which can be interpreted as an unknown light vector boson [5]. The vector boson (X) is observed as a resonance in e^+e^- pairs whose invariant mass is $m_X = 16.7 \pm 0.35_{\text{stat}} \pm 0.5_{\text{sys}}$ MeV. If one supposes a purely vector interaction between the Standard Model matter fields and the light vector boson, the consistency in the other experimental results requires the interaction should be protophobic [6, 7], which can be written as

$$\mathcal{L}_{\text{int}} = -X_\mu (g_u \bar{u} \gamma^\mu u + g_d \bar{d} \gamma^\mu d + g_e \bar{e} \gamma^\mu e + g_\nu \bar{\nu}_L \gamma^\mu \nu_L), \quad (1)$$

where

$$\begin{aligned} 2.0 \times 10^{-4} &\lesssim |g_u| \lesssim 1.0 \times 10^{-3}, \\ 4.0 \times 10^{-4} &\lesssim |g_d| \lesssim 2.0 \times 10^{-3}, \\ 6.1 \times 10^{-5} &< |g_e| < 4.2 \times 10^{-4}, \\ |g_\nu g_e|^{1/2} &\lesssim 9.1 \times 10^{-5} \text{ (for } g_\nu g_e < 0), \\ |g_\nu g_e|^{1/2} &\lesssim 2.1 \times 10^{-5} \text{ (for } g_\nu g_e > 0). \end{aligned} \quad (2)$$

The coupling with the neutron g_n , which is defined as $g_n = g_u + 2g_d$, satisfies $6.1 \times 10^{-4} \lesssim |g_n| \lesssim 3.0 \times 10^{-3}$. On the other hand, the coupling with proton $g_p (= 2g_u + g_d)$ is restricted as $|g_p| \lesssim 3.6 \times 10^{-4}$. We fix the couplings as $g_n = 3.0 \times 10^{-3}$, $g_p = 0$, $g_e = 4.2 \times 10^{-4}$, and $g_\nu = 0$ in

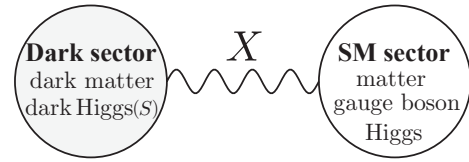


FIG. 1. A schematic description of models considered in this Letter.

the following discussion. Phenomenology of the X boson and their models have been investigated in Refs. [7–9].

In this Letter, we assume the light vector boson to be a gauge boson of a broken $U(1)_X$ gauge symmetry and to be a mediator between the Standard Model and the dark sector which includes the dark matter, as in Fig. 1. Using some simple models, we investigate experimental constraints on their parameters in the dark sector, and also discuss the compatibility with the thermal relic dark matter scenario.

MODELS OF $U(1)_X$ CHARGED DARK MATTERS

As the dark sector, we consider a spontaneous symmetry breaking of the $U(1)_X$ gauge symmetry by a dark Higgs S , which is a complex scalar boson charged under $U(1)_X$. The Lagrangian of the dark sector is

$$\begin{aligned} \mathcal{L}_X &= -\frac{1}{4} X^{\mu\nu} X_{\mu\nu} + (D_\mu S)^\dagger (D^\mu S) + \mu_S^2 |S|^2 - \frac{\lambda_S}{2} |S|^4 \\ &= -\frac{1}{4} X^{\mu\nu} X_{\mu\nu} + \frac{m_X^2}{2} X^\mu X_\mu + \frac{1}{2} (\partial_\mu s)^2 - \frac{m_s^2}{2} s^2 \\ &\quad + g_X m_X s X^\mu X_\mu - \frac{g_X m_s^2}{2m_X} s^3 + \dots, \end{aligned} \quad (3)$$

where $X^{\mu\nu}$ is the field strength tensor of X . The scalar field S is expanded as $S = (v_s + s)/\sqrt{2}$ in the unitarity gauge, and $D_\mu S = (\partial_\mu + ig_X X_\mu)S$. Some terms irrelevant in our computation are suppressed here. The parameters are defined as

$$v_s^2 = 2\mu_S^2/\lambda_S, \quad m_s^2 = \lambda_S v_s^2, \quad m_X = g_X v_s. \quad (4)$$

The original parameters μ_S and λ_S can be written by m_X and m_s with the gauge coupling g_X . For simplicity, we consider that interactions between the Higgs boson and the dark sector can be neglected [10].

First, we study a complex scalar and a Dirac fermion dark matter models, where the dark matters are charged under $U(1)_X$. If the dark matter is the complex scalar field φ , the Lagrangian is

$$\mathcal{L}_\varphi = |(\partial_\mu + ig_\varphi X_\mu)\varphi|^2 - m_\varphi^2 |\varphi|^2 - \frac{\lambda_\varphi}{2} |\varphi|^4 - \lambda_{\varphi S} |\varphi|^2 |S|^2 + \mathcal{L}_X. \quad (5)$$

Since the annihilation into ss and XX are the s-wave processes, they dominate the thermal relic abundance. In this model, the experimental bounds on these two channels are, in addition to the dark matter mass m_φ , determined by the couplings $\lambda_{\varphi S}$ and g_φ , respectively.

The annihilation cross section at the dark age ($m_{\text{DM}}/T \sim 3 \times 10^{12}$) is bounded by an observation of the cosmic microwave background (CMB) by the Planck as $\langle\sigma v\rangle/m_{\text{DM}} \lesssim 1.0 \times 10^{-27} \text{cm}^3/\text{s}/\text{GeV}$ [15, 16]. Hence, the region where the dark matter is lighter than 30 GeV is naively excluded by the result. Even if the dark matter is heavier than the value, the large Sommerfeld enhancement through the X boson excludes the thermal relic scenario [17, 18]. The similar bound is obtained by AMS-02 for the region $m_\varphi > 10 \text{ GeV}$ [19, 20] with $m_{\text{DM}}/T \sim 3 \times 10^6$. These indirect signals are 1- or 2-step cascades studied in Ref. [21]. The region is also excluded by the direct detection result of the LUX experiment [22]. In order to see these bounds, we have followed the analysis method used in Refs. [23–25]. These results are shown in Fig. 2.

For simplicity, we consider only the XX channel in the figure, so that, only g_φ is relevant coupling. The result can be translated into the ss channel with the replacement of g_φ^2 by $\lambda_{\varphi S}/(2\sqrt{2})$ in their non-relativistic annihilation cross sections. Even if the both of the channels contribute to the annihilation process, the thermal relic dark matter cannot be obtained. Note that recently Ref. [9] has shown that if the dark matter is lighter than the vector boson a certain parameter region can explain the thermal relic abundance, see Fig. 2.

Considering the Dirac fermion dark matter ξ , the Lagrangian is

$$\mathcal{L}_\xi = \bar{\xi}(i\cancel{\partial} - g_\xi \cancel{X} - m_\xi)\xi + \mathcal{L}_X, \quad (6)$$

where ξ is the dark matter. The dark matter annihilates through the s-wave processes into XX and sX . The situation of the experimental bounds and the consequence for the thermal relic scenario are the same with φ , except for the light dark matter window. The non-relativistic annihilation cross section of $\xi\bar{\xi} \rightarrow XX$ is just a half of the cross section of $\varphi\varphi^* \rightarrow XX$ if $g_\xi = g_\varphi$, while the result of the sX channel is give by the replacement of g_ξ^2 with

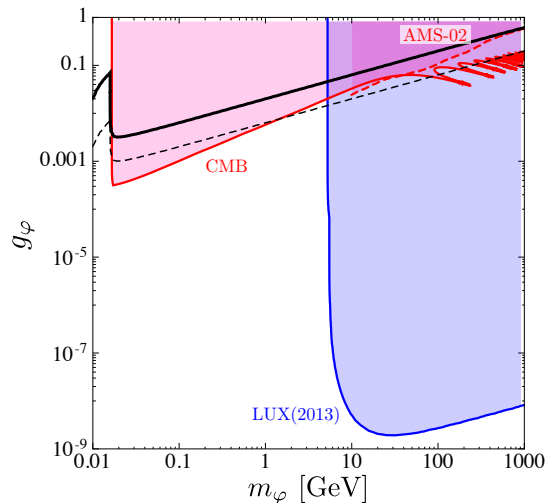


FIG. 2. The experimental constraints on the gauge coupling g_φ as a function of the dark matter m_φ . The solid black line means the observed dark matter abundance, namely, $\langle\sigma v\rangle = 6 \times 10^{-26} \text{cm}^3/\text{s}$ with $x = 20$. On the dotted black line, the dark matter abundance is the two order of magnitudes larger than the abundance. The red regions are excluded by the Planck and the AMS-02 experiments, while the blue region has been excluded by the LUX experiment.

$g_\xi g_X/2$. Since the Sommerfeld enhancement factor is the same with φ , the result is almost the same as Fig. 2, so that the thermal relic scenario is also excluded.

MODELS OF SECLUDED DARK MATTERS

Next, we study the $U(1)_X$ singlet dark matter models. Interactions between the dark matters and the Standard Model are induced by the mixing with another particle charged under the $U(1)_X$ gauge symmetry.

In the case of the real scalar dark matter ϕ , the dark Higgs s can be used as the mediator. After the spontaneous symmetry breaking, the Lagrangian is

$$\mathcal{L}_\phi = \frac{1}{2}(\partial^\mu \phi)^2 - \frac{m_\phi^2}{2} \phi^2 - \frac{\lambda_{\phi S} m_X}{2g_X} s\phi^2 - \frac{\lambda_{\phi S}}{4} s^2 \phi^2 - \frac{\lambda_\phi}{4!} \phi^4 + \mathcal{L}_X, \quad (7)$$

where we impose a Z_2 symmetry ($\phi \leftrightarrow -\phi$) to stabilize the dark matter. The coupling $\lambda_{\phi S}$ is introduced like $\lambda_{\varphi S}$.

In the previous section, the direct detection excludes the thermal relic scenario if the dark matters is heavier than about 5 GeV. In this model, however, the leading contribution to the direct detection comes from the loop induced diagram shown in Fig. 3. Hence, the direct detection bound becomes significantly weaker than the previous models.

Since the scalar three point interaction is proportional to m_X , the Sommerfeld enhancement factor is also suppressed by m_X/m_ϕ [26], unless $\lambda_{\phi S} \gg g_X$.

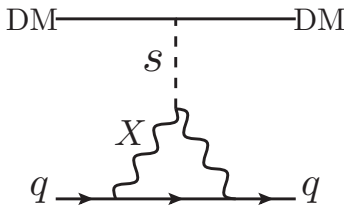


FIG. 3. The leading contribution of the direct detection in the $U(1)_X$ singlet dark matters.

We also consider the $U(1)_X$ singlet dark matter model including a Majorana fermion χ . Since the Majorana fermion can not interact with S alone, we additionally introduce a Dirac fermion ψ whose $U(1)_X$ charge is the same with S . Then, the Lagrangian is

$$\mathcal{L}_\chi = \bar{\psi}(i\cancel{\partial} - g_X \cancel{X} - m_\psi)\psi + \frac{1}{2}\bar{\chi}(i\cancel{\partial} - m_\chi)\chi - y(S\bar{\psi}\chi + S^\dagger\bar{\chi}\psi) + \mathcal{L}_X, \quad (8)$$

where the Yukawa coupling y can be chosen as real and positive without loss of generality. After the spontaneous symmetry breaking, the coupling becomes the source of the fermion mixing. The mass eigenstates are obtained by a $SO(3)$ rotation and a chiral rotation to flip the sign of a mass term as

$$\begin{aligned} \mathcal{L}_\chi &\supset -\frac{1}{2}(\bar{\chi}^c \bar{\psi}_1^c \bar{\psi}_2^c) \begin{pmatrix} m_\chi & \frac{y v_s}{\sqrt{2}} & \frac{y v_s}{\sqrt{2}} \\ \frac{y v_s}{\sqrt{2}} & 0 & m_\psi \\ \frac{y v_s}{\sqrt{2}} & m_\psi & 0 \end{pmatrix} \begin{pmatrix} \chi \\ \psi_1 \\ \psi_2 \end{pmatrix} + \text{H.c.} \\ &= -\frac{1}{2}(\bar{\eta}_1^c \bar{\eta}_2^c \bar{\eta}_3^c) \begin{pmatrix} m_1 & 0 & 0 \\ 0 & m_2 & 0 \\ 0 & 0 & m_3 \end{pmatrix} \begin{pmatrix} \eta_1 \\ \eta_2 \\ \eta_3 \end{pmatrix} + \text{H.c.} \quad (9) \\ &= -\frac{1}{2}m_i \bar{\chi}_i \chi_i, \quad (10) \end{aligned}$$

where ψ_1 and ψ_2 are, respectively, the left-handed and the charge conjugation of the right-handed components in ψ , namely, $\psi_2 = (\psi_R)^c$. The mass eigenstates χ_i are the four component Majorana fermions defined as $\chi_i = (\eta_i, \eta_i^c)^T$. We assign the mass eigenvalues so as to be $0 < m_1 < m_2 < m_3$, i.e., the dark matter is χ_1 . Then, the Lagrangian is written as follows,

$$\mathcal{L}_\chi = \frac{1}{2}\bar{\chi}_i((i\cancel{\partial} - m_i)\delta^{ij} - g^{ij}\cancel{X} - y^{ij}s)\chi_j + \mathcal{L}_X, \quad (11)$$

where

$$\begin{aligned} g^{ij} &= g_X \begin{pmatrix} 0 & -i\sqrt{\frac{m_3-m_2}{m_3-m_1}} & 0 \\ i\sqrt{\frac{m_3-m_2}{m_3-m_1}} & 0 & i\sqrt{\frac{m_2-m_1}{m_3-m_1}} \\ 0 & -i\sqrt{\frac{m_2-m_1}{m_3-m_1}} & 0 \end{pmatrix}, \quad (12) \\ y^{ij} &= y \begin{pmatrix} -2\sqrt{\frac{(m_3-m_2)(m_2-m_1)}{m_3-m_1}} & 0 & \frac{m_3-2m_2+m_1}{m_3-m_1} \\ 0 & 0 & 0 \\ \frac{m_3-2m_2+m_1}{m_3-m_1} & 0 & 2\sqrt{\frac{(m_3-m_2)(m_2-m_1)}{m_3-m_1}} \end{pmatrix}. \quad (13) \end{aligned}$$

The mass eigenvalues are related as

$$m_3 - m_2 = \frac{y^2 m_X^2}{g_X^2 (m_2 - m_1)}. \quad (14)$$

In the numerical analyses below, we chose $m_2 - m_1 = 100$ GeV to evade the complexity of the co-annihilation of the dark fermions.

The leading contribution to the direct detection signal is also the loop diagram given in Fig. 3 like the real scalar model. Since the s-wave annihilation channel is suppressed by $m_X^4/(m_2 - m_1)^4$, the leading annihilation process is the p-wave. Hence, the indirect detection bound does not work to exclude the thermal relic scenario for the Majorana dark matter.

Even though the indirect detection bounds are too weak, the Sommerfeld enhancement factor [27] and the self-scattering cross section can be large if one takes the region of the heavy dark matter mass m_1 and the lighter mediator mass m_s . In this situation, the large self-interaction can solve the small scale structure problems as shown in the next section.

PHENOMENOLOGY OF THE REAL SCALAR DARK MATTER

We show the indirect and the direct detection bounds of the real scalar dark matter model, and that whether they are compatible with the thermal relic abundance or not. We also investigate future prospects of the direct detection bound.

The dark Higgs s mediates the annihilation into the X pair and the direct detection as Fig. 3. In these processes, amplitude can be written without g_X . Since the annihilation to ss is almost insensitive to g_X , the physics of this model is described by only $\lambda_{\phi S}$ and the dark matter mass. Indeed, our results are not changed in $g_X = \mathcal{O}(0.01-1)$.

As we have shown in Fig. 4, since the Sommerfeld enhancement is suppressed, the CMB bound excludes the thermal relic scenario only if the dark matter is lighter than about 30 GeV. The electron-positron flux excludes the scenario up to the mass of about 100 GeV.

In this Letter, we consider the case that the masses of the X boson and the dark Higgs bosons are the same scale. Note that because the transfer momentum in the dark matter-nucleon scattering in Fig. 3 is also the same scale $\mathcal{O}(10-100)$ MeV, therefore the transfer-momentum contribution to the direct detection is not neglected. In addition to the LUX bound in 2013 [22], we have also drawn their recent result [28], and the prospects of the XENON1T [29] and the LZ experiments [30]. Evaluating the hadronic matrix elements, we have used a result of the lattice QCD simulation [31]. It is found that the current LUX bound is too weak to exclude the thermal relic scenario. The expected bound by LZ can exclude the scenario up to a few hundreds GeV, for $m_s = 50$ MeV.

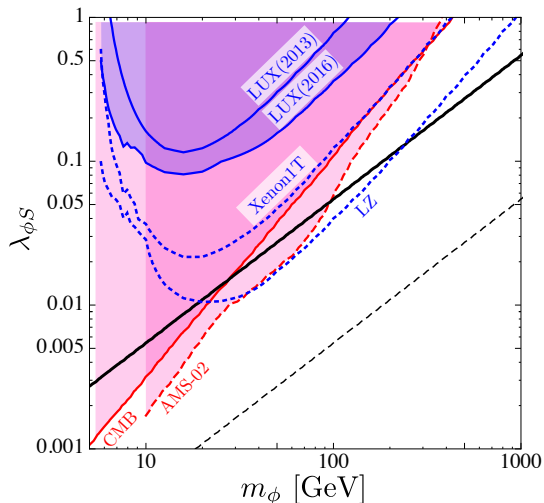


FIG. 4. The constraints on the coupling between the dark Higgs and the dark matter $\lambda_{\phi S}$ as a function of the dark matter mass with $m_s = 50$ MeV. The blue/red region is bounded by the current direct/indirect dark matter searches. The projected direct detection bounds by the XENON1T and the LZ experiments are shown with the blue dotted lines. On the solid black line, the dark matter satisfies the observed thermal relic abundance $\langle\sigma v\rangle = 3 \times 10^{-26}$ cm³/s with $x = 20$. On the dotted black line, the dark matter thermal relic density is one hundred times larger than the one.

The dark Higgs mass dependence of the expected direct detection bounds is shown in Fig. 5. It is found that the expected bounds by the XENON1T and the LZ experiments can exclude the scenario up to 200 GeV and above 1 TeV, respectively. If the dark Higgs is lighter than the X boson, the scalar decays via two off-shell states. In the case, a loop induced decay into $e\bar{e}$ becomes the dominant channel. Eventually, the life time of the dark Higgs becomes larger than one second, so that the observed matter abundance could be suffered if the dark Higgs abundance is too large. The direct detections can reach the higher dark matter mass for the lighter dark Higgs. Considering the life time of the dark Higgs, the reaches decrease about 100 GeV.

PHENOMENOLOGY OF THE MAJORANA DARK MATTER

Since the Majorana dark matter mainly annihilates through the p-wave process, only the direct detection is important to restrict the thermal relic scenario. The bounds and the prospects are shown in the Fig. 6.

The Yukawa coupling to obtain the thermal relic abundance becomes large, when the dark matter is heavier than the mass difference $m_2 - m_1$. Below the value, the cross section is determined by the mass difference, so that the coupling is independent of the dark matter mass. Recently, the region heavier than about 40 GeV has been excluded for $m_s = 50$ MeV. With the projected experi-

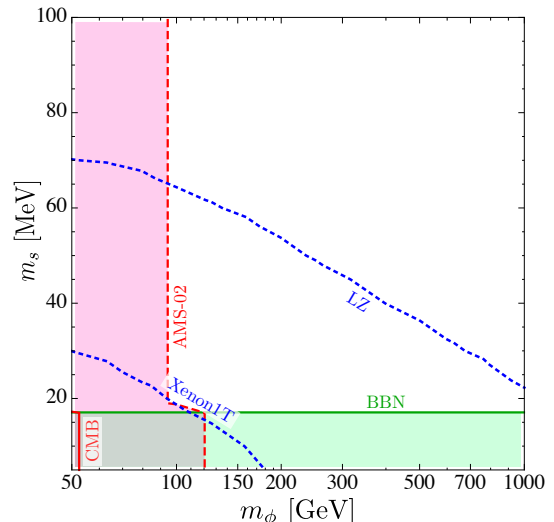


FIG. 5. The dark Higgs mass dependence of the expected direct detection bounds. The coupling $\lambda_{\phi S}$ is chosen to satisfy the thermal relic abundance. The blue dotted lines are the projected direct detection bounds. The red region is excluded by the indirect detections. In the green region, the life time of the dark Higgs is larger than one second.

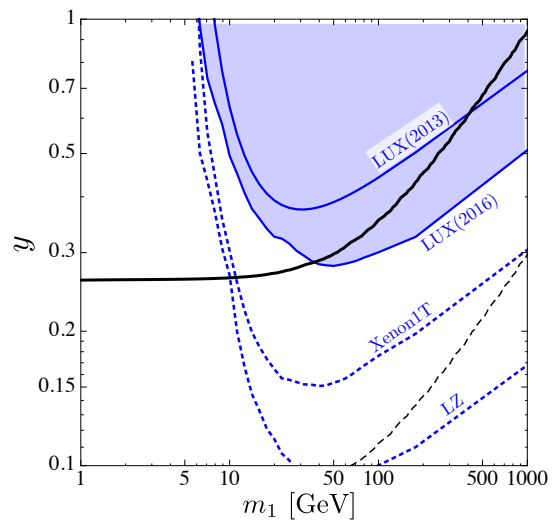


FIG. 6. The constraints of the Yukawa coupling and the mass for the Majorana dark matter. The vertical axis is the Yukawa coupling y . The other objects are the same with Fig. 4.

ments, the thermal relic region is excluded until the lower limit of their sensitivity, i.e., $m_1 \sim 10$ GeV. Similar to the real scalar dark matter case, these behavior are almost independent of g_X .

Considering the heavy dark Higgs, the direct detection bound becomes weaker. The current bound is not sensitive if $m_s > 100$ MeV, while the prospected sensitivities by the XENON1T and the LZ experiments reach the dark Higgs of 200 and 350 MeV, respectively.

As mentioned before, the self-scattering cross section is enhanced by $m_X^4 m_1^2 / (g_X m_s (m_2 - m_1))^4$. We have calculated the velocity-averaged transfer cross section

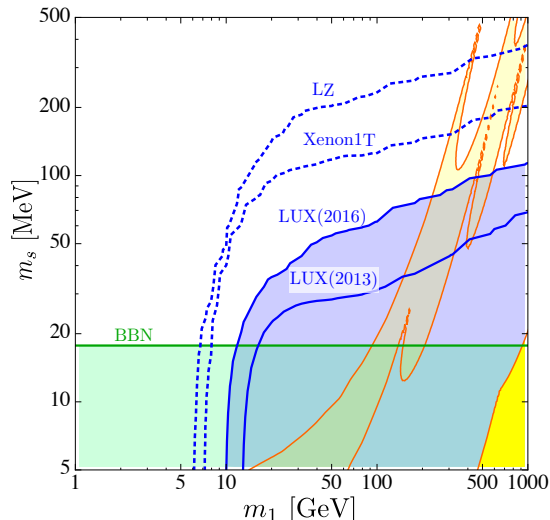


FIG. 7. The m_s dependence of the several constraints for the thermal relic Majorana dark matter. The self-scattering cross section to solve the small scale structure puzzle, i.e., $0.1 \leq \langle \sigma_T \rangle / m_1 \leq 10 \text{ cm}^2/\text{g}$, is also shown in yellow (lighter yellow) band for $g_X = 10^{-2}$ (10^{-3}). The others are same with Fig. 5.

[32], and found that due to the enhancement, the self-interaction can be large enough to solve the small scale structure puzzles. In this case, the coupling g_X should be a bit smaller than 10^{-2} . The details are shown in Fig. 7.

CONCLUSION AND DISCUSSION

In this Letter, we have investigated the dark matter models where the photophobic 16.7 MeV boson is a mediator between the Standard Model and the dark sector.

Because of the severe constraint from the CMB observation, due to the large Sommerfeld enhancement, the thermal relic scenarios are almost excluded in the $U(1)_X$ charged dark matter models.

Considering the spontaneous symmetry breaking of the $U(1)_X$ gauge symmetry, it is found that, when the dark matter is the $U(1)_X$ singlet, the dark matter can easily satisfy the observed relic abundance under the current experimental constraints. Some parameter regions can be probed by the future direct detection experiments. Particularly, in the Majorana dark matter model, the large self-scattering cross section to solve the small scale structure puzzles can be achieved, while a bit small g_X is required.

According to Ref. [3], a light and a long-lived particle could solve the Lithium problem. Hence, the parameter region where the dark Higgs becomes a long-lived particle also attracts our attention [33].

ACKNOWLEDGMENTS

The work of Y.Y. is supported in part by JSPS KAKENHI Grant Number 15K05053. The author Y.Y. thanks

M. Tanaka and R. Watanabe for useful comments.

* teppey.kitahara@kit.edu

† yamayasu@het.phys.sci.osaka-u.ac.jp

- [1] M. Pospelov, A. Ritz and M. B. Voloshin, *Phys. Lett. B* **662** (2008) 53 [arXiv:0711.4866 [hep-ph]].
- [2] M. Kaplinghat, S. Tulin and H. B. Yu, *Phys. Rev. Lett.* **116**, no. 4, 041302 (2016) [arXiv:1508.03339 [astro-ph.CO]].
- [3] A. Goudelis, M. Pospelov and J. Pradler, *Phys. Rev. Lett.* **116**, no. 21, 211303 (2016) [arXiv:1510.08858 [hep-ph]].
- [4] M. Endo, K. Hamaguchi and G. Mishima, *Phys. Rev. D* **86** (2012) 095029 [arXiv:1209.2558 [hep-ph]].
- [5] A. J. Krasznahorkay *et al.*, *Phys. Rev. Lett.* **116**, no. 4, 042501 (2016) [arXiv:1504.01527 [nucl-ex]].
- [6] J. L. Feng, B. Fornal, I. Galon, S. Gardner, J. Smolinsky, T. M. P. Tait and P. Tanedo, *Phys. Rev. Lett.* **117** (2016) no.7, 071803 [arXiv:1604.07411 [hep-ph]].
- [7] J. L. Feng, B. Fornal, I. Galon, S. Gardner, J. Smolinsky, T. M. P. Tait and P. Tanedo, arXiv:1608.03591 [hep-ph].
- [8] P. H. Gu and X. G. He, arXiv:1606.05171 [hep-ph]; L. B. Chen, Y. Liang and C. F. Qiao, arXiv:1607.03970 [hep-ph]; Y. Liang, L. B. Chen and C. F. Qiao, arXiv:1607.08309 [hep-ph].
- [9] L. B. Jia and X. Q. Li, arXiv:1608.05443 [hep-ph].
- [10] The couplings between the dark sector and the Higgs boson are introduced as $\lambda_{SH}|S|^2|H|^2$ and $\lambda_{\varphi H}|\varphi|^2|H|^2$. The Higgs to the dark Higgs pair decay has four electron-positron pairs in the final state. In order to suppress the significant contribution to the total width of the Higgs, since the current bound is five times larger than the Standard Model prediction, the coupling λ_{SH} should be smaller than about 0.06, see Ref. [11, 12]. The coupling $\lambda_{\varphi H}$ is constrained by the direct detection and direct measurement of the Higgs invisible width as a Higgs portal dark matter. Roughly speaking, the coupling should be smaller than about 0.01 to evade any experimental bound, see Ref. [13, 14].
- [11] G. Aad *et al.* [ATLAS Collaboration], *Eur. Phys. J. C* **75** (2015) no.7, 335 [arXiv:1503.01060 [hep-ex]].
- [12] V. Khachatryan *et al.* [CMS Collaboration], *Phys. Rev. D* **92** (2015) no.7, 072010 [arXiv:1507.06656 [hep-ex]].
- [13] S. Kanemura, S. Matsumoto, T. Nabeshima and N. Okada, *Phys. Rev. D* **82** (2010) 055026 [arXiv:1005.5651 [hep-ph]].
- [14] J. M. Cline, K. Kainulainen, P. Scott and C. Weniger, *Phys. Rev. D* **88** (2013) 055025 Erratum: [*Phys. Rev. D* **92** (2015) no.3, 039906] [arXiv:1306.4710 [hep-ph]].
- [15] P. A. R. Ade *et al.* [Planck Collaboration], arXiv:1502.01589 [astro-ph.CO].
- [16] M. Kawasaki, K. Nakayama and T. Sekiguchi, *Phys. Lett. B* **756** (2016) 212 [arXiv:1512.08015 [astro-ph.CO]].
- [17] J. Hisano, S. Matsumoto, M. M. Nojiri and O. Saito, *Phys. Rev. D* **71**, 063528 (2005) [hep-ph/0412403].
- [18] S. Cassel, *J. Phys. G* **37**, 105009 (2010) [arXiv:0903.5307 [hep-ph]].

- [19] L. Accardo *et al.* [AMS Collaboration], *Phys. Rev. Lett.* **113**, 121101 (2014).
- [20] M. Aguilar *et al.* [AMS Collaboration], *Phys. Rev. Lett.* **113**, 121102 (2014).
- [21] G. Elor, N. L. Rodd, T. R. Slatyer and W. Xue, *JCAP* **1606** (2016) no.06, 024 [arXiv:1511.08787 [hep-ph]].
- [22] D. S. Akerib *et al.* [LUX Collaboration], *Phys. Rev. Lett.* **112**, 091303 (2014) [arXiv:1310.8214 [astro-ph.CO]].
- [23] M. I. Gresham and K. M. Zurek, *Phys. Rev. D* **89**, no. 1, 016017 (2014) [arXiv:1311.2082 [hep-ph]].
- [24] T. Li, S. Miao and Y. F. Zhou, *JCAP* **1503**, no. 03, 032 (2015) [arXiv:1412.6220 [hep-ph]].
- [25] E. Del Nobile, M. Kaplinghat and H. B. Yu, *JCAP* **1510**, no. 10, 055 (2015) [arXiv:1507.04007 [hep-ph]].
- [26] A. Hryczuk, *Phys. Lett. B* **699**, 271 (2011) [arXiv:1102.4295 [hep-ph]].
- [27] A. Hryczuk, R. Iengo and P. Ullio, *JHEP* **1103**, 069 (2011) [arXiv:1010.2172 [hep-ph]].
- [28] D. S. Akerib *et al.*, arXiv:1608.07648 [astro-ph.CO].
- [29] E. Aprile [XENON1T Collaboration], *Springer Proc. Phys.* **148**, 93 (2013) [arXiv:1206.6288 [astro-ph.IM]].
- [30] D. S. Akerib *et al.* [LZ Collaboration], arXiv:1509.02910 [physics.ins-det].
- [31] A. Abdel-Rehim *et al.* [ETM Collaboration], *Phys. Rev. Lett.* **116**, no. 25, 252001 (2016) [arXiv:1601.01624 [hep-lat]].
- [32] S. Tulin, H. B. Yu and K. M. Zurek, *Phys. Rev. D* **87**, no. 11, 115007 (2013) [arXiv:1302.3898 [hep-ph]].
- [33] T. Kitahara and Y. Yamamoto, in preparation.